Accepted Manuscript

A nanostructural view of the cell wall disassembly process during fruit ripening and postharvest storage by atomic force microscopy

Sara Posé, Candelas Paniagua, Antonio J. Matas, A. Patrick Gunning, Victor J. Morris, Miguel A. Quesada, José A. Mercado

PII: S0924-2244(17)30567-8

DOI: 10.1016/j.tifs.2018.02.011

Reference: TIFS 2169

To appear in: *Trends in Food Science & Technology*

Received Date: 31 August 2017

Revised Date: 6 February 2018

Accepted Date: 12 February 2018

Please cite this article as: Posé, S., Paniagua, C., Matas, A.J., Gunning, A.P., Morris, V.J., Quesada, M.A., Mercado, J.A., A nanostructural view of the cell wall disassembly process during fruit ripening and postharvest storage by atomic force microscopy, *Trends in Food Science & Technology* (2018), doi: 10.1016/j.tifs.2018.02.011.

This is a PDF file of an unedited manuscript that has been accepted for publication. As a service to our customers we are providing this early version of the manuscript. The manuscript will undergo copyediting, typesetting, and review of the resulting proof before it is published in its final form. Please note that during the production process errors may be discovered which could affect the content, and all legal disclaimers that apply to the journal pertain.

ACCEPTED MANUSCRIPT

A nanostructural view of the cell wall disassembly process during fruit ripening and postharvest storage by atomic force microscopy

Sara Posé[1], Candelas Paniagua[1*], Antonio J. Matas[1], A. Patrick Gunning[2], Victor J. Morris[2], Miguel A. Quesada[3], José A. Mercado[1]

[1]Instituto de Hortofruticultura Subtropical y Mediterránea "La Mayora" (IHSM-UMA-CSIC), Departamento de Biología Vegetal, Universidad de Málaga, 29071 Málaga, Spain

[2]Quadram Institute of Bioscience, Norwich Research Park, Colney, Norwich NR4 7UA, UK

[3]Departamento de Biología Vegetal, Universidad de Málaga, 29071 Málaga, Spain

Corresponding author:

José A. Mercado

Instituto de Hortofruticultura Subtropical y Mediterránea "La Mayora" (IHSM-UMA-CSIC), Departamento de Biología Vegetal, Universidad de Málaga, 29071 Málaga, Spain

e-mail: mercado@uma.es

*Present address: Centre for Plant Science, School of Biology, University of Leeds, UK

ACCEPTED MANUSCRIPT

ACCEPTED MANUSCRIPT

ABSTRACT

Background: The mechanical properties of parenchyma cell walls and the strength and extension of adhesion areas between adjacent cells, jointly with cell turgor, are main determinants of firmness of fleshy fruits. These traits are modified during ripening leading to fruit softening. Cell wall modifications involve the depolymerisation of matrix glycans and pectins, the solubilisation of pectins and the loss of neutral sugars from pectin side chains. These changes weaken the cell walls and increase cell separation, which in combination with a reduction in cell turgor, bring about textural changes. Atomic force microscopy (AFM) has been used to characterise the nanostructure of cell wall polysaccharides during the ripening and postharvest storage of several fruits. This technique allows the imaging of individual polymers at high magnification with minimal sample preparation.

Scope and approach: This paper reviews the main features of the cell wall disassembly process associated to fruit softening from a nanostructural point of view, as has been provided by AFM studies.

Key findings and conclusions: AFM studies show that pectin size, ramification and complexity is reduced during fruit ripening and storage, and in most cases these changes correlate with softening. Postharvest treatments that improve fruit quality have been proven to preserve pectin structure, suggesting a clear link between softening and pectin metabolism. Nanostructural characterisation of cellulose and hemicellulose during ripening has been poorly explored by AFM and the scarce results available are not conclusive. Globally, AFM could be a powerful tool to gain insights about the bases of textural fruit quality in fresh and stored fruits.

Keywords: atomic force microscopy, cell wall, hemicellulose, fruit softening, fruit texture, pectins, postharvest

1. Introduction

Fleshy fruits represent an important component of human and animal diet as a source of fibre, minerals, and phytonutrients. Fruit are also an important source of cell wall polysaccharides, specially pectins, used in food industry as modifiers of food products and/or as dietary supplements with health benefits (Harris & Smith, 2006). Recently, by-products and wastes of fruit industry has received attention as a source of biomaterials, e.g. 3D-matrices for cell culture (Munarin et al., 2011), cell delivery vehicles (Neves et al., 2015), bionanocomposites for food-packaging (Oliveira et al., 2017). As a group, fleshy fruits have a varied botanical origin; however, all of them undergo a genetically controlled program of tissue differentiation, fruit ripening that includes the production of aromatic compounds, colour changes and flesh softening. The final ripe product is an edible fruit which promotes seed dispersal. Fruit ripening is a major physiological process for the reproduction of flowering plants, and from an agricultural point of view, is also a key process which confers positive qualities to the fruit, making them marketable and palatable for human consumption. As stated before, fruits develop changes in texture during ripening but the over softening, and subsequent increased pathogen susceptibility, leads to important postharvest spoilage and economic losses. Therefore, the inhibition or delay of these negative consequences of fruit ripening remains a major challenge to breeders and fruit physiologists.

In the market, texture is the principal fruit quality attribute (Goulao & Oliveira, 2008), being firmness and juiciness the most important textural properties for the consumers (Toivonen & Brummell, 2008). The definition of texture is complex because entails several attributes which determine the feel of food within the mouth and also the way these attributes can be measured (Harker, Stec, Hallett & Bennett, 1997; Bourne, 2002). Fleshy fruits have been classified in two texture categories, those that develops a melting texture at ripe stage, with a short postharvest life and a poor relationship between firmness at harvest and after storage (e.g. peach, apricot, melon, plum, kiwifruit, tomato, strawberry) and those that soften moderately and preserve a crisp, fracturable texture as they ripen, with longer storage life and a close relationship between firmness at harvest and after storage (e.g. apple, quince, nashi pear, cranberry, watermelon) (Mercado, Pliego-Alfaro & Quesada, 2011).

Texture of fleshy fruits is a complex trait which depends on shape, size and turgor of parenchyma cells (closely related to cell wall thickness and strength), the extension and strength of adhesion areas between adjacent cells, which mostly relies on the middle lamella, and the presence of non-parenchyma cells, most of which containing thickened walls (epidermal cells, vascular elements, fibers and sclereids) (Harker et al., 1997). During ripening, the disassembly of parenchyma cell walls modifies their mechanical properties and the dissolution of the middle lamella reduces cell adhesion. These modifications, together with a loss of turgor pressure, lead to fruit juiciness and softening (Harker et al., 1997; Toivonen & Brummell, 2008) (Fig. 1). In fruits with thick and well developed cuticles such as tomato or grape, the decrease of turgor may be a primary cause of softening (Saladié et al., 2007; Castellarin et al., 2016).

The disassembly of cell wall polymers and the dissolution of the middle lamella during fruit softening are mainly promoted by the coordinated action of cell wall degrading enzymes or

proteins, involving more than 50 cell wall structure related genes (Goulao & Oliveira, 2008; Mercado et al., 2011; Gapper, McQuinn & Giovannoni, 2013). The non-enzymatic degradation of cell wall pectins by hydroxyl radicals oxidation has also been suggested (Airianah, Vreeburg & Fry, 2016). How cell wall polysaccharides entangles to form the highly dynamic structure that shaped plant cells is still largely unknown and a deeper knowledge about polysaccharide structure and composition is critical to understand the process of fruit softening.

Atomic force microscopy (AFM) has been traditionally used in food science as an imaging tool to study food macromolecules and colloids (Gunning & Morris, 2017). In recent years, this technique has also been employed to study a complex biological process such as fruit ripening, focusing mainly in the role of pectin modifications during fruit softening (Paniagua et al., 2014). The major focus of this review is to summarise the insights gained through AFM on the structural features of cell wall polysaccharides and their modifications during fruit ripening and postharvest, to correlate cell wall nanostructural characteristics with the mechanical properties of the fruit.

2. Cell wall composition, structure and analysis

Fleshy fruit tissues are mainly formed by parenchyma cells with a thin primary wall. In dicotyledonous and some monocotyledonous, Type I primary cell wall comprises a load-bearing cellulose-matrix glycan framework embedded in a more soluble matrix of pectic polysaccharides, joint with small amounts of glycoproteins, low-molecular weight compounds and ions (Willats, McCartney, Mackie & Knox, 2001). Composition of primary cell wall in dicot plants consists in 30% each of cellulose, matrix glycans and pectins, plus a 1-10% of structural proteins. However, pectins can account up to 60% of cell wall mass in fleshy fruits (Redgwell et

al. 1997a; Prasanna, Prabha & Tharanathan, 2007). Fruit cell walls have also a high water content.

Cellulose, the main component of the cell wall, is constituted by a linear chain of 500 to 7500 β-(1-4) linked D-glucose monomers. Several cellulose chains (more than 30 parallel chains) associate by hydrogen bonds to constitute microfibrils. The matrix glycans, also known as hemicelluloses, include a group of neutral or weakly acidic polysaccharides characterized by (1→4)-β- linked backbones of glucose (Glc), xylose (Xyl) or mannose (Man), decorated with neutral or slightly acid sugar side chains (Scheller & Ulvskov, 2010). The most abundant hemicellulosic component in dicot is xyloglucan (XyG), linear chains of (1→4)-β-D-glucose with numerous Xyl units linked at regular sites to the O-6 position of Glc units. Xyloglucans bind tightly to the surface of the cellulose microfibrils by hydrogen bonds and are long enough to span the 20-40 nm distance between adjacent microfibrils, linking them together forming a network (Park & Cosgrove, 2012).

Pectins, polymers largely composed of D-galacturonic acid (GalA), are among the most complex macromolecules found in nature (Voragen, Coenen, Verhoef & Schols, 2009) and this complexity is very well reflected in all their biological functions; in the middle lamella, where polyuronides are the main component, regulate cell adhesion (Willats et al., 2001); in the primary cell wall, these polymers conform a highly hydrated matrix that determines wall porosity, provides charged surfaces that modulate pH and ion balance, and they are the source for different signalling molecules involved in many biological responses, including fruit ripening. Pectins are a source of soluble and insoluble fibre, as well as functional ingredient in processed foods. In addition to the health benefits of dietary fibre, new health claims have emerged, related to the bio-active roles of modified pectins as anti-cancer agents (Morris,

Gromer, Kirby, Bongaerts & Gunning, 2011; Maxwell, Belshaw, Waldron & Morris, 2012). These polysaccharides are also important in the food industry as gelling and thickening agent (Sila et al., 2009).

Pectins are distributed in three main domains: homogalacturonan (HG), rhamnogalacturonan I (RGI) and rhamnogalacturonan II (RGII). HG is the most abundant pectin, accounting for 50-90% of total polyuronide amount in cell walls (Yapo, 2011a). This polymer is formed by a linear backbone of 100-200 GalA units linked by α-(1→4) glycosidic bonds. The HG is synthesized in the Golgi as a high methyl-ester at the C-6 carboxyl residues, and deposited in the cell wall with a 70-80% degree of methyl-esterification (Willats et al., 2001) plus lower degrees of additional acetylation on O-3 or O-2 at the same or different GalA residues. De esterification of methyl groups allows pectin gel formation through the parallel cross-link of HG chains by calcium in a multipolymer assembly called egg-box structure. Xylogalacturonans (XGA), substituted-HG with single xylose residues and/or small xylose side chains, 2-8 resides, are also abundant in storage tissues of reproductive organs (Yapo, 2011a). RGI are highly ramified pectins formed by a backbone of the disaccharide (1→2)-α-L-rhamnose-(1→4)-α-D-galacturonic acid, with 20-80% of rhamnose residues substituted at O-4 or O-3 positions with arabinan, galactan or arabinogalactan side chains (Willats et al., 2001; Yapo, 2011b). The number of lateral residues varies from a single glycosyl residue to 50 or more, producing a highly variable family of polysaccharides. RGI polyuronides are frequently known as hairy regions in comparison with the smooth region of HG. Finally, RGII is a branched polymer composed of 9 GalA residues containing four heteropolymeric side chains with more than 20 uncommon sugar residues, which glycosyl sequence is highly conserved in all vascular plants (Matsunaga et al., 2004; O'Neill, Ishii, Albersheim & Darvill, 2004). RGII is present in the cell wall as dimers covalently cross-

linked by a borate diester. Most of the RGII domains *in muro* are dimerised by tetrahedral B-bridges involving the O-2 and O-3 apiosyl residues of side chain A in each RGII monomer (O'Neill et al., 2004; Yapo, 2011a; Chormova, Messenger & Fry, 2014).

Despite the chemistry and basic structure of each pectin family is well established, there are several hypothetical models about how pectin domains are interconnected: i) the "smooth and hairy regions" model shows the pectin as a HG linear backbone, interspersed with rhamnosyl residues, alternated with branched RGI regions (Voragen et al., 2009); ii) the "RGI backbone model" suggests that RGI is the main pectin backbone, and linear HG would be side chains of the RGI core (Vincken et al., 2003); iii) the more complex "living-thing like" model depicts the pectin as a RGI backbone connected with two unbranched HG blocks at the extremes (Yapo, 2011a); iv) a more recent model shows pectin as a HG domain, unbranched or with few number of HG branches, linked to a RGI core of lower length (Paniagua et al., 2017a). The localization of the different pectin domains *in muro* is also unknown. HG is generally believed to be surrounding the cells, with the calcium pectate confined to the middle lamella and cell corners; RGI would be located in the primary cell wall, likely coating microfibril surfaces to interlink both, pectin and cellulose-glycan cell wall networks; RGII seems to be widespread in the wall except in the middle lamella (Vincken et al., 2003).

As occur for pectin domains, interactions among the different cell wall components and its spatial localization *in muro* are still under debate. Classically, the "tethered network model" shows XyG coating the surface of separated microfibrils and spanning the distance between adjacent microfibrils, while pectic polymers is an independent phase embedding the cellulose-XyG network (Park & Cosgrove, 2012). This model emphasizes the XyG tethers as key determinants of cell wall biomechanics. However, some experimental results, such as the almost

184 normal phenotype of an *Arabidopsis* mutant deficient in XyG (Cavalier et al., 2008), the failure
185 of xyloglucan-specific endoglucanase to induce cell wall creep in hypocotyls (Park & Cosgrove,
186 2012), the evidences of direct pectin-cellulose crosslinks (Zykwinska, Thibault & Ralet, 2008;
187 Wang, Park, Cosgrove & Hong, 2015), or the key role of pectinase enzymes in texture of some
188 fruits (Atkinson et al., 2012; Posé et al., 2015; Uluisik et al., 2016) have challenged this
189 hypothesis. Park and Cosgrove (2012) proposed a novel model suggesting the presence of
190 regions of close contact between cellulose microfibils, referred as biomechanical "hot spots",
191 mediated by XyG, together with a major occurrence of pectin-cellulose interactions than
192 previously hypothesized.

193 As regards cell wall analysis, most studies involve the isolation and purification of its
194 components by solubilisation in extractants of increasing astringency. The first step usually
195 involves the use of solvents to prevent endogenous enzyme degradation of fruit tissue
196 homogenates and isolate cell wall extracts, like boiling alcohols or phenol based solutions. Once
197 cell wall material is isolated, the residue is sequentially extracted by solutions of increasing
198 astringency to produce fractions enriched in a specific wall component. Usually these solutions
199 are (1) water, yielding pectins freely soluble in the apoplast and solubilized by *in vivo* processes
200 (Redgwell, Melton & Brasch, 1992); (2) chelating agents, e.g. imidazole or trans-1,2-
201 diaminocyclohexane-N,N,N'N'-tetraacetic acid (CDTA), solubilizing pectins ionically bound to
202 the cell wall; (3) a weak alkali like sodium carbonate, releasing pectins covalently bound to the
203 primary wall; (4) dilute and concentrated strong alkalis (e.g. sodium or potassium hydroxide at
204 1M and 4M), solubilizing matrix glycans loosely and tightly bound to the cell wall, respectively;
205 (5) and cellulose solvents (e.g. cadoxen) to solubilize matrix glycans and pectins imbricated into
206 the amorphous surface of cellulose microfibrils. The residue after this sequential extraction is

mainly composed by pure cellulose. Although these cell wall fractions are based on their different chemical solubility, they are still representative of particular polymers moieties *in muro*. Thus, first solutions (phenol and water) extracts polysaccharides that are readily soluble or poorly bound to the matrix; chelating agents extract pectins rich in HG from middle lamella; mild alkalis like Na_2CO_3 extracts pectins covalently bound to the wall and enriched in neutral sugars, probably from the primary cell wall; strong alkalis solubilise xyloglucans. Main drawback of this method is the disruption of some bonds during the extraction, so the structural integrity of the wall is lost. Alternatively, *in situ* analysis of the cell wall can be performed by different analytical techniques (Vicente, Saladié, Rose & Labavitch, 2007a). AFM has also been applied on cell walls *in situ* (Routier-Kierzkowska et al., 2012; Kafle et al., 2014), although most results gathered until now using this microscope are from the analysis of isolated cell wall fractions and these will be the main focus in this review.

3. Cell wall disassembly is one of the major determinant factor of fruit shelf life

Softening during fruit ripening is mainly associated with the dissolution of the middle lamella and the modification of the composition and structure of polymers present in the primary cell wall (Brummell, 2006; Goulao & Oliveira, 2008; Mercado et al., 2011). In general, the cell wall disassembly process involves the depolymerisation of matrix glycans, the solubilisation and depolymerisation of pectins and the loss of neutral sugars from pectin side chains (Fig. 1). The extension of these changes varied greatly among different fruits (Mercado et al., 2011), and, in general, no one of these processes fully correlates with the softening event.

Cell wall and cellulose content slightly decrease during ripening in most fruits, although cellulose cristallinity is not significantly altered during ripening or in fruit cultivars of

contrasting firmness (Koh, Melton & Newman, 1997; Newman and Redgwell, 2002; Ng et al., 2014). Depolymerisation of loosely or tightly bound XyG is common to many fruits and, according to Brummell (2006), this is the cell wall modification that most closely correlate with softening. In peach, XyG depolymerisation is one of the early events during softening (Brummell, Del Cin, Crisosto & Labavitch, 2004). However, some fruits, such as apple or papaya, ripen in the absence of XyG depolymerisation (Percy, Melton & Jameson, 1997; Shiga et al., 2009), and in soft fruits such as raspberry and strawberry, this process is absent or cultivar dependent (Rosli, Civello & Martinez, 2004; Vicente, Ortugno, Powell, Greve & Labavitch, 2007b). Additionally, functional analyses of genes encoding endo-β-1-4-glucanases, which substrates are thought to be XyG, glucomannans and integral and peripheral regions of non-crystalline cellulose (Brummell & Harpster, 2001), have failed to found any significant effect of gene suppression or overexpression in fruit softening (reviewed in Mercado et al., 2011).

Although the contribution of XyG depolymerisation to fruit softening is controversial, the rearrangement and/or disentanglement of the cellulose-XyG network seems to play a major role in this process. The loss of the structural integrity of the XyG matrix due to the action of specific xyloglucan endotransglycosylase/hydrolase (XTH) enzymes has been suggested as a primary cause of softening (Miedes, Herbers, Sonnewald & Lorences, 2010). The XTH genes encode proteins that can potentially have XyG endo-transglycosidase activity, non-hydrolytic cleavage and ligation of XyG chains, and endo-hydrolase activity, yielding irreversible chain degradation (Eklöf & Brumer, 2010). XTH comprise a large gene family with temporal- and tissue-specific expression patterns, playing distinct roles in the cell wall (Eklöf and Brumer, 2010). Recently, two groups of XTH genes have been identified in persimmon (Han et al., 2017) and apple (Zhang et al., 2017a), one involved in the maintenance of the cell wall during fruit growth and

253 the other one involved in the cell wall disassembly during fruit ripening. Expansins are a second
254 group of proteins that alter the cellulose-XyG network. These proteins disrupt non-covalent
255 interactions between hemicelluloses and cellulose microfibrills promoting cell wall loosening
256 and extension. In most fruits analysed, expansins are encoded by multigene families whose
257 members show different expression pattern, being either related to the fruit growth or to the
258 ripening process (Mercado et al., 2011). Evidences for a key role of expansin in fruit softening
259 have been obtained by the manipulation of *SlExp1* gene expression in tomato, both in transgenic
260 plants (Brummell et al., 1999) and in mutants induced by TILLING (Minoia et al., 2016). The
261 suppression of this gene moderately increased fruit firmness, whereas transgenic overexpression
262 increased softening. However, these texture phenotypes were not linked to the same modification
263 of the cell wall. The increased firmness was related to a lower depolymerisation of chelated
264 pectins in the transgenic suppressed plants (Brummell et al., 1999) but to a modification of
265 hemicellulose structure in the TILLING mutants (Minoia et al., 2016). By contrast, the increased
266 softening of *SlExp1* overexpressed was associated to a higher xyloglucan depolymerisation early
267 in ripening, without affecting pectin depolymerisation (Brummell et al., 1999). Therefore, the
268 role of expansins in softening remains uncertain.

269 Pectin are extensively modified during fruit ripening, being subjected to solubilisation and, in
270 several fleshly fruits, also depolymerisation. Pectin solubilization comprises an increase in the
271 content of pectins loosely bound to the cell wall, mainly those extracted with phenol-acetic acid-
272 water (PAW) or water, and in some cases also chelated pectins, which takes place in parallel to a
273 decrease in the amount of covalently bound pectins (Paniagua et al., 2014). Apparently, pectin
274 solubilisation occurs at the expense of polyuronides more tightly linked to the walls (Brummell,
275 2006). The disentanglement of the pectin network may also facilitate the swelling of the cell wall

due to the penetration of water into enlarged intermicrofibrillar spaces (Redgwell et al., 1997a). This process would allow increased mobility of wall enzymes within cell wall matrix and increased accessibility of hydrolytic enzymes to their substrates (Brummell, 2006). Pectin solubilisation could be directly related with the texture of ripe fruits, since those fruits with a melting texture, such as avocado, kiwifruit, blackberry, tomato, persimmon, melon, peach or strawberry, show a high to moderate solubilisation, while in those fruit with a crisp texture at ripening, eg. apple, watermelon or nashi pear, pectin solubilisation is low or undetectable (Mercado et al., 2011). Even in this last type of fruits, a lower pectin solubilisation has been associated to lower softening rates in cultivars of contrasting softening behavior (Ng et al., 2015).

The reasons for the solubilisation of pectins are unclear and several hypotheses have been proposed. Neutral side chains from RGI might anchor pectins to the wall either by physical entanglement with other wall polymers or by binding to matrix glycans and cellulose (Zykwinska et al., 2008). The marked loss of arabinose and galactose detected during the ripening of many fruits (Redgwell et al., 1997b), could weaken the pectin network. It is noteworthy that the silencing of a β-Galactosidase gene reduces fruit softening in strawberry (Paniagua et al., 2016). It has been suggested that Gal loss takes place mostly in arabinogalactan pectins loosely bound to XyG (Paniagua et al., 2016). However, neutral sugar loss and pectin solubilisation does not correlate in some fruits; for example, plum shows extensive solubilisation with no loss of arabinose or galactose, while apple and nashi pear display an extensive loss of galactose but very slight pectin solubilisation (Redgwell et al., 1997b).

Depolymerisation of chelated and/or covalently bound pectins might also cause solubilisation although this process is not as general as polyuronide solubilisation. Additionally, pectin

depolymerisation usually takes place at later stages of ripening (Mercado et al., 2011). Some fruits display a substantial loss of high molecular weight polyuronides, e.g. avocado, tomato, peach, kiwifruit (Redgwell et al., 1997a; Brummell et al., 2004), while others display low to moderate depolymerisation of bound pectins, e.g. strawberry, blueberry, melon, apple (Redgwell et al., 1997a; Rose, Hadfield, Labavitch & Bennett, 1998; Vicente et al., 2007b; Paniagua et al., 2017b). Depolymerisation is also lower in non-melting peach cultivars when compare with melting cultivars (Yoshioka, Hayama, Tatsuki & Nakamura, 2011). Suppression of pectinase gene expression reduces softening in fruits with quite different textural properties. In strawberry, a soft fruit, the downregulation of a pectate lyase or a polygalacturonase gene, both cleaving glycosidic bonds of demethylesterified HG but with different enzymatic mechanisms, resulted in fruits significantly firmer than the control at the ripe stage (Jiménez-Bermúdez et al., 2002; Quesada et al., 2009). Cell wall of transgenic fruits showed less depolymerisation of bound pectins as well as a lower degree of pectin solubilisation (Santiago-Doménech et al., 2008; Posé et al., 2013). Although earlier works only found minor effects of polygalacturonase antisense silencing on tomato fruit firmness, a recent report indicates that pectate lyase also plays a key role on softening in this fruit (Uluisik et al., 2016). Pectin depolymerisation by polygalacturonases also seems to determine firmness in fruits with a crisp texture like apple (Atkinson et al., 2012).

During ripening, many fruits undergo a progressive demethylesterification of HG induced by the expression of pectin methylesterase genes (Prasanna et al., 2007; Goulao & Oliveira, 2008). This pectin modification might create large regions of negatively charged side groups which would contribute to the loosening of pectins by electrostatic repulsion (Brummell, 2006). However, functional studies of pectin methylesterase genes failed to find an effect of these genes

on fruit firmness (Wen, Ström, Tasker, West & Tucker, 2013). The synthesis of more freely soluble forms of pectins as the fruit ripens and the degradation of the RGI backbone by rhamnogalacturonases (Molina-Hidalgo et al., 2013) have also been suggested to explain pectin solubilisation.

Besides ripening, processing fruit into different food products substantially alters cell wall polysaccharide structure and subsequently the mechanical properties of the product. Technological processes aiming to alter the texture of processed fruits, which has been called "texture/rheology engineering", are mainly focused on pectin changes (Sila et al., 2009; Van Buggenhout, Sila, Duvetter, Loey & Hendrickx, 2009).

Summarising, both hemicellulose and pectin networks are modified during ripening although the mechanisms involved in these processes are largely unknown. Functional analyses of ripening specific genes encoding cell wall proteins point out to the disentanglement of pectins as a major event regulating fruit firmness and shelf life. However, this hypothesis should be taken with care since these assays have been carried out in a limited number of species. The characterization of primary walls at the nanostructural level by AFM would shed light on how cell wall polymers are processed during softening. The potential of this approach to provide better knowledge of fruit ripening is discussed in the next sections.

4. AFM analysis of cell wall disassembly during fruit ripening

4.1 AFM fundamentals

The use of AFM in food science started shortly after its invention and nowadays is a well-established technology in this field. Instead of optical lenses, AFM relies on a sharp tip that raster the surface of the sample to renders topographical images at molecular level. Briefly, the

tip is mounted on a flexible cantilever that act as a spring and deflects over the roughness of surfaces; a piezoelectric device controls the movements and force exerted by the tip and allows the nanometric adjustment in real time to keep both tip and sample in a very close contact during the scan. The nanoscale movements are transduced and amplified by a laser beam deflection over an optical quadrant, and further amplified and converted to topographical images by a computer connected in line. More details about the AFM setup and operational modes are described elsewhere (Morris, Kirby & Gunning, 2010). AFM sample preparation is minimal and can be performed either on air or liquid which allows AFM scanning under physiological conditions, rendering a perfect match between AFM and research in Biology. Figure 2 shows schematically main applications of AFM in the study of fruit ripening. Particularly important is the ability of AFM to identify isolated single polymers in a sample due to its unique imaging acquisition through the measurement of spatial parameters in three dimensions. Thus, the topographical information of AFM images allows the differentiation between true branch points or superpositions of two molecules, just checking the height value at the apparent branch point, which will remain the same as the main backbone height in case of true branch points (Round, Rigby, MacDougall, Ring & Morris, 2001).

An increasing application of AFM is its capacity to probe forces at nanometer scale. This microscope can be used as a “molecular force inducer” to analyse molecular binding features between molecules or large colloidal particles (Gunning & Morris, 2017). Also as a force transducer, AFM could be used as a “cellular texturometer”, able to probe *in vivo* plant tissue mechanics at cellular level. This application, named cellular force microscopy (Routier-Kierzkowska et al., 2012), is able to simultaneously assess and manipulate tissue mechanics.

Despite its potential, the AFM assessment of molecular binding among cell wall polymers has been poorly explored.

Until now, cell walls from a variety of fruits have been visualised by AFM, resolving nanostructural conformation (height, length, branching, polymer aggregation) of its isolated cell wall polysaccharides. The structural data at nanoscale add new cues about the potential role of each cell wall component in the fruit mechanical properties. A summary of these studies is shown in Table 1.

4.2 Nanostructural analysis of fruit cellulose and matrix glycans

Few AFM data about the disentanglement of the cellulose-hemicellulose network or the disassembly of hemicellulose during fruit softening are available. These polymers have mainly been studied in growing tissues such as hypocotyl or coleoptiles. In these organs, cellulose microfibrils appear as wavy but mostly parallel ordered fibers (Ding et al., 2012; Kafle et al., 2014). Recently, Zhang, Zheng and Cosgrove (2016) observed in different vegetative tissues that microfibrils were not crosslinked but some of them were almost grazed in some points of the matrix, supporting the biomechanical "hot spots" hypothesis suggested by Park and Cosgrove (2012).

The relationship between cellulose microfibrils properties, diameter and crystallinity, and fruit texture is unclear. Cybulska, Zdunek, Psonka-Antonczyk & Stokke (2013) observed that apple cultivars with crisper, harder and juicier fruits had thicker microfibrils of lower crystallinity than softer cultivars. By contrast, AFM images of cellulose assemblies in two different pear cultivars with contrasting firmness revealed microfibrils of similar diameter, around 23 nm, in both cases (Zdunek, Koziol, Cybulska, Lekka & Pieczywek, 2016). Another works in onion and maize

cellulose microfibrils reported diameters of 3-4 nm approximately, a value in accordance with the dimensions of the 36-chain cellulose elementary fibril model, using high resolution AFM (Ding et al., 2012; Zhang et al., 2016). Additionally, ultrathin microfibril diameters, in the range of 1-2 nm, has been reported in soft tissues like leaves, flower petals, or fruits, including peach and strawberry, where microfibrils were isolated by mild alkaline extraction in order to preserve its native structure (Niimura, Yokoyama, Kimura, Matsumoto & Kuga, 2010). Thimm, Burritt, Ducker & Melton (2009) observed that the mean size of celery microfibrils increased as pectins and hemicelluloses were selectively removed, not only as result of the swelling of the microfibrils but also to an increase on the tendency to self-associate forming aggregates. Thus, special attention to *in vivo* or never-dried cell walls, or mild extraction methods need to be addressed in order to avoid inconclusive and contradictory data, and evaluation of cellulose microfibrils in the closer to nature environment as possible is advisable.

The appearance of hemicellulose polysaccharides under AFM might be strongly influenced by the extraction procedure and/or the commodity under study. Chen et al. (2009) showed that the hemicelluloses from Chinese cherries extracted with $NaOH/NaBH_4$ after cell wall depectination with CDTA looked like a broom, with long main chains, 2-5 µm, including many branches that were about 100 nm to 2 µm. However, a treatment of the cell wall with potassium oxalate and later extraction of hemicellulose resulted in dissociated hemicellulose chains. In pear, hemicelluloses extracted with 1M KOH had a rod-like shape with 1-4 nm height and lengths in the range of 20-800 nm (Zdunek, Koziol, Pieczywek & Cybulska, 2014). Samples of minimally processed xyloglucans from *Tamarindus indica* L. seeds are also visualized as helicoidal fibres of 2.3 nm diameter and 640 nm length (Koziol, Cybulska, Pieczywek & Zdunek, 2015). As occurred for cellulose, comparative studies of hemicellulose nanostructure in fruits with

413 contrasting texture did not detect clear differences. Chen et al. (2009) observed that a cherry
414 cultivar with crisp texture contained a higher percentage of thicker hemicellulose chains than the
415 softer one. By contrast, Zdunek et al. (2014) suggested that the improved texture of the pear cv.
416 'Xenia' when compared with the softer cv. 'Conference' could be related with thinner and more
417 flexible hemicellulose chains which could facilitate cellulose crosslinking and increase cell wall
418 stiffness.
419
420 *4.3 AFM has provided a novel view of pectin structure*
421 Pectin is the cell wall component most studied by AFM (Table 1). Visualisation of pectin
422 samples isolated from fruits has revealed a great nano-structural heterogeneity as a mixture of
423 linear chains, branched chains and pectin complexes or aggregates. Examples of these structures
424 can be observed in Figs. 3 and 4. Since neutral sugars are present as much shorter chains, not
425 detected by AFM, it has been postulated that long branches in linear chains would be composed
426 by HG (Round et al., 2001). Thus, AFM has gathered evidences of the non-canonical GalA as
427 side branches of HG, named galacturonogalacturonan (GaGA), challenging the traditional view
428 of HG as linear unbranched GalA chains. Although some studies described a small percentage of
429 HG with GalA branch point residues, its low occurrence has probably prevented the inclusion of
430 GaGA in pectin models. Ovodova et al. (2006) described a branched HG, with acid residues
431 attached to 2-O- and 3-O-positions of the GalA residues of the galacturonan backbone, in marsh
432 cinquefoil by AFM and methylation analysis. Round, Rigby, MacDougall & Morris (2010) also
433 suggested an acidic nature for the side chains of HG in tomato pectins, supported by AFM
434 images of samples subjected to mild acid hydrolysis, sugar composition and linkage analyses.
435 More recently, Paniagua et al. (2017a) observed that length of both, pectin backbone and

436 branches, diminished after digestion of sodium carbonate pectin samples with fungal endo-PG.
437 An indirect evidence of the GalA nature of HG side branches has been obtained in transgenic
438 strawberry lines with a polygalacturonase or a pectate lyase gene downregulated, both enzymes
439 having demethylesterified HG as target. Transgenic pectin samples obtained from ripe fruits
440 showed a higher percentage of branched molecules than control, suggesting a correlation
441 between HG degradation and an acidic nature for side branches (Pose et al., 2015). Although the
442 chemical nature of the branch point is unknown, AFM evidences of the existence of GalA as side
443 branches of HG should be included as another feature of fine pectin structure in future models.

444 Early AFM works in unripe tomato fruit showed pectins extracted by CDTA and sodium
445 carbonate as linear chains with a branching degree of 30%, some of them being multi-branched,
446 in both pectin fractions (Round, MacDougall, Ring & Morris, 1997; Round et al., 2001). The
447 backbone length ranged between 30 to 390 nm fitting a log-normal distribution, being the chains
448 in the CDTA fraction 3-fold longer than those extracted with sodium carbonate (Round et al.,
449 2001; Kirby, MacDougall & Morris, 2008). Regarding branching, branch length had a narrower
450 range (30-170 nm). Similar results have been obtained in pectins from apple (Zareie, Gokmen &
451 Javadipour, 2003) and strawberry fruits (Pose, Kirby, Mercado, Morris & Quesada et al., 2012).
452 In this last species, both CDTA and sodium carbonate pectins showed a similar percentage of
453 branched polymers (8-9%), although covalently bound pectins displayed more branches per
454 backbone (Posé et al., 2012). Lengths of isolated pectin chains visualized by AFM in different
455 fruits are in accordance with the degree of polymerization of HG deduced with different
456 analytical techniques (Paniagua et al., 2014).

457 AFM data of pectin chain heights are in the range 0.5-2 nm, which is in accordance with a
458 helix structure of chains with different aggregation status (Yang, Chen, An & Lai, 2009), since

459 the vertical height of single-stranded polysaccharides is 0.5 nm (McIntire & Brant, 1999).
460 Comparison of chain width values obtained by AFM among the different reports is not suitable
461 due to the probe broadening effect, i.e. as the radius of the AFM tip is larger than the diameter of
462 the molecules being measured, the image of the molecule is convoluted with the tip profile and
463 the measured dimension is considerably overestimated (Morris et al., 2010). Thus, a wide range
464 of pectin width values, in the range 15-230 nm, have been reported in different fruits (Paniagua
465 et al., 2014). Probe broadening effect might also explain the discrepancy between pectin height
466 and width values. However, some authors suggested a natural aggregation of pectins based on
467 numerical regularities in the widths of pectin chains, so that any chain width could be obtained as
468 the sum of some of these basic values. For instance, three (54, 72 and 91 nm) or four (11.7, 15.6,
469 19.5 and 35.1 nm) basic width values have been reported in peach by Zhang et al. (2012) and
470 Yang, An, Feng, Li and Lai (2005), respectively. Evidences of pectin assemblies have also been
471 obtained in carrot, where Cybulska, Zdunek and Koziol (2015) found that sodium carbonate
472 pectins have the ability of self-organize into an ordered network. In some fruits, e.g. peach (Yang
473 et al., 2009), jujube (Wang et al., 2012) or apricot (Liu et al., 2017), much larger pectin fibers, 1-
474 3 µm length, have been observed. Recently, Mierczyńska, Cybulska & Zdunek (2017) reported
475 the comparison of pectins from different fruits. AFM images showed plum pectins as long, thick
476 and branched molecules that resembles long pectins observed in peach (Yang et al., 2009),
477 jujube (Wang et al., 2012) and apricot (Liu et al., 2017); however, pectin from raspberry and
478 strawberry appears mostly like thinner fibres highly interconnected in a network, that resemble
479 previous images from strawberry (Pose et al., 2012) and tomato (Kirby et al., 2008). Similar long
480 fibrous pectins have previously been reported in strawberry, especially in unripe fruits (Fig. 5),
481 although these structures were recognized as a possible artifact of the extraction procedure (Pose

et al., 2012). In general, fruits with long pectin chains (longer than 1000 nm) share a consistent texture of relatively high firmness, in comparison with strawberry, tomato or raspberry, with thinner and shorter pectin chains, that are characterized by a strong softening during ripening. Apart from the sample and preparation method, further analyses are needed to support the *in muro* occurrence of pectin supramolecules of high degrees of pectin assembly.

In the other hand, micelle-like aggregates of several sizes, frequently with long chains arising from the central core, are generally visualized in AFM samples of fruit pectins (Kirby et al., 2008; Pose et al., 2012). The size of the complexes decreased upon mild acid hydrolysis, a treatment that release neutral sugars, although remnants of these complexes persisted after prolonged hydrolysis (Round et al., 2010). These results suggest that the globular core of the aggregates could be composed by RGI and HG, and their arising linear chains would be made of HG and/or poorly or short-branched RGI (Round et al., 2010). In this line, a recent molecular modelling analysis of RGI has suggested an extended threefold helical structure for its backbone and an antiparallel pairing of galactan side chains, which would be a new way of non-covalent pectin cross-link (Makshakova, Gorshkova, Mikshina, Zuev, & Perez, 2017). These links might facilitate the formation of the complexes observed by AFM. RGII could also be involved in the stabilization of the micellar aggregates. This molecule forms dimers via borate diester bridges between RGII belonging to two different layers of HG. Paniagua et al. (2017b) observed that the removal of borate ester cross-linking without altering glycosidic linkages reduced in an 80% the number of pectin aggregates visualized in strawberry samples. Further studies are needed to corroborate the chemical composition of such micellar macromolecules.

In summary, most nanostructural data on fruit pectins obtained by AFM analysis are in agreement with our previous knowledge on these polysaccharides, supporting the reliability of

505 this approach in the study of cell wall disassembly during fruit softening. Additionally, AFM has
506 provided novel cues to understand the way in which the different pectin domains might assemble
507 *in muro*, either in the form of self-assembled pectin fibres or micellar aggregates.
508
509 *4.4 Structural modifications of pectins during fruit ripening and postharvest*
510 AFM has been used to describe nanostructural modifications of cell wall polymers during
511 fruit ripening and postharvest storage, with a focus on pectins as the most dynamic component of
512 cell wall during this process. In Chinese cherry (Zhang et al., 2008), tomato (Xin et al., 2010)
513 and Chinese jujube (Wang et al., 2012) differences in structure of chelated pectins between
514 ripening stages have been detected, being pectins from unripe fruit longer and wider than those
515 from ripe fruit. Recently, Paniagua et al. (2017b) analysed CDTA and sodium carbonate pectin
516 fractions in unripe and ripe strawberry fruits. Quantitative analysis of AFM images showed that
517 CDTA samples from unripe fruits were longer, while no changes were detected in the sodium
518 carbonate fraction. Interestingly, a general decrease in the percentage of chain ramifications and
519 the number of pectin aggregates from unripe to ripe stage was detected, which nicely correlates
520 mechanical features (fruit firmness) with pectin complexity (debranching and aggregation).
521 In some species, the comparison of ripe fruits from cultivars of contrasting texture shows a
522 positive correlation between pectin length and firmness. Yang et al. (2009) analysed water,
523 chelated and covalently-bound pectins in two peach cultivars with soft and crisp texture. The
524 most significant difference between the two cultivars was detected in the covalently bound
525 pectins, that were longer and more branched in the crisp fruit, suggesting that differences in
526 texture in peach could be mainly related to the neutral-sugar-rich pectin fraction from the
527 primary cell wall. In the case of pear cultivars with contrasting texture, no differences were

528 observed for water soluble pectin fraction. However, the firmer cultivar possesses thicker and
529 more branched pectin molecules at the chelated fraction and a denser network for bound pectins
530 (Zdunek et al., 2014). Additionally, pear pectin fractions treated with pectinases revealed that
531 degradation of pectin nanostructure was closely related with softer cell walls, and it was
532 hypothesized that this could be due to the creation of new pores and the increase in pore size of
533 the pectin matrix (Koziol, Cybulska, Pieczywek & Zdunek, 2017). Contrary to peach, the length
534 of pectins from two Chinese cherry cultivars of contrasting firmness did not correlate with
535 texture and wider but shorter pectin chains from the sodium carbonate fraction were observed in
536 the firmest cultivar (Zhang et al., 2008).

537 An increasing number of studies have used AFM to characterize pectin modifications during
538 postharvest storage. The reduction of fruit firmness in peach stored at low temperatures was
539 associated to a decrease in the amount of covalently bound pectins, which were shorter and
540 thinner when increasing storage time and temperature (Zhang et al., 2010). Additionally, most
541 pectins formed large aggregates in fresh fruits that were reduced during the storage period. A
542 similar result was observed in water- and CDTA-soluble pectins, although chelated pectins in
543 fruits at harvest were visualized mainly as single linear chains with a small number of aggregates
544 (Zhang et al., 2012). The lengths of soluble and covalently bound pectins from strawberries
545 decreased by 30-39% during storage of the fruit at low temperature for 15 days (Chen et al.,
546 2011). Treatments that extends postharvest life in some commodities, such as controlled
547 atmospheres or application of $CaCl_2$, reduced the structural degradation of pectins in peach
548 (Yang et al., 2005; Yang, Lai, An & Li, 2006a; Yang, Feng, An & Li, 2006b), apricot (Liu et al.,
549 2017) and strawberry (Chen et al., 2011). Vacuum impregnation with calcium lactate has also
550 been successfully applied in papaya to preserve its texture during postharvest; texture

551 improvements were correlated with a lower degradation of chelated pectins (Yang, Wu, Ng &
552 Wang, 2017). The use of coatings has positive effects on the preservation of fruit quality
553 attributes on several fruits. In the case of honeydew melon, AFM analysis showed the
554 stabilization of bound pectins after coating with chitosan combined with calcium chloride
555 (Chong, Lai & Yang, 2015). Similar preservation of nanostructure of covalently bound pectins
556 has been reported for chitosan combined with nano-SiOx particle coatings in Chinese cherry
557 (Xin, Chen, Lai & Yang, 2017). A rice bran coating has been successfully applied to extend
558 postharvest life of cherry tomatoes and the beneficial effects of this treatment correlated with a
559 lower degradation of chelated pectins (Zhang et al., 2017b). Altogether, the nanostructural
560 analysis of pectins by AFM in several fruits supports a key role of pectin nanostructure in fruit
561 softening and postharvest shelf life.
562
563 *4.5 Nanomechanical analysis of fruit cell walls by AFM*
564 As described in previous sections, fruit cell walls undergo extensive changes in structure and
565 composition during ripening and postharvest storage that reduce their mechanical strength,
566 favouring softening. The mechanical properties in plant tissues can be measured at different
567 scales (from macro to nano), being the nano-scale the most recommendable for a proper analysis
568 of stiffness of the cell wall, middle lamella, polysaccharides and even linkages within the cell
569 wall. Measurements of cell wall stiffness, quantitatively described by the Young´s or elasticity
570 module, could contribute to understand the process of fruit softening. Unfortunately, few studies
571 have addressed this issue.
572 Several methods have been developed to measure the cell wall stiffness at micrometer
573 dimension. Micro-compression, micro-penetration or micro-indentation tests have been

574 performed to measure individual living cells and tissues (Routier-Kierzkowska et al., 2012;
575 Burgert & Keplinger, 2013). However, cell wall thickness requires more sensitive methods to
576 allow a proper estimation of the stiffness. Nano-indentation using AFM could solve this
577 problem, allowing measurement at sub-micro and nano-scale (Zdunek & Kurenda, 2013). In this
578 technique, the AFM tip is pushed into the surface of the sample with a specific force and force-
579 indentation curves, which represents the approach and retraction of the cantilever to the sample,
580 are collected (Burgert & Keplinger, 2013; Gunning & Morris, 2017). The data obtained are
581 converted by mathematical models into physic parameters, such as Young´s module, to describe
582 the elasticity or stiffness of the sample (Gunning & Morris, 2017). Stiffness values of
583 parenchyma fruit cells obtained with this technique are highly variable, e.g. 100 KPa in tomato
584 cells incubated in Murashige and Skoog medium (Zdunek & Kurenda, 2013), 0.6 MPa in apple
585 cells isolated in a solution of sodium carbonate plus mannitol (Cárdenas-Pérez et al., 2016) or 77
586 MPa in grape cells suspension cultured in Nitsch-Nitsch medium (Lesniewska, Adrian, Klinguer
587 & Pugin, 2004). It should be considered that indenter geometry, turgor pressure and internal
588 stresses have a significant impact on the Young´s module values obtained with AFM (Burgert &
589 Keplinger, 2013; Zdunek & Kurenda, 2013). In a recent study, Zdunek et al. (2016) measured
590 stiffness of cell wall fragments isolated from pear cultivars of contrasting firmness during pre-
591 harvest and postharvest storage. Alcohol-insoluble cell wall residues were used to avoid the
592 contribution of the cell turgor. A positive correlation between cell wall stiffness and fruit
593 firmness was found during pre-harvest in both cultivars; however, after postharvest storage,
594 Young´s modulus of the primary cell walls increased whereas fruit firmness decreased.
595 Additionally, no clear differences in cell wall stiffness between both cultivars were observed
596 despite their differences in texture. The reasons for the discrepancy between mechanical

properties at macro and nano-scale levels are unknown. Zdunek et al. (2016) suggested that the increase on cell wall stiffness during postharvest could be related to the degradation of covalently linked pectins as the fruit soften, since negative correlations among Young´s modulus and galacturonic acid content in bound pectin fractions were found. However, Koziol et al. (2017) observed a linear decrease of Young´s modulus in cell walls from pears after sequential removing of pectins. Apple tissue subjected to ultrasounds also showed a decrease in cell wall stiffness that was paralleled to an increase in galacturonic acid in all cell wall pectin fractions (Pieczywek, Koziol, Konopacka, Cybulska & Zdunek, 2017). The degree of pectin methylesterification and the availability of Ca^{2+} ions, both factors influencing the formation of cross-linked pectin gels, could also contribute to the reduction of tissue stiffness, as has been observed in the zones of organ initiation in meristems (Peaucelle et al., 2011) or in onion epidermal cells (Xi, Kim & Tittmann, 2015). Although the relationship between pectin solubilisation and cell wall stiffness remains unclear these evidences show that both parameters are closely related.

5. Concluding remarks

Softening during fruit ripening and postharvest storage is a complex process which fundamental bases are still largely unknown. Cell wall disassembly, mediated by the expression of ripening specific genes encoding cell wall proteins, is generally considered as the main factor determining softening although the role of turgor and water loss could be a key component of softening for some fruits. These processes induce cell wall loosening leading to the modification of fruit texture. Recent evidences are challenging our traditional view of the cellulose-hemicellulose network as the load-bearing framework determining mechanical properties of the

cell wall, providing a more relevant role to the pectin matrix. Along this line, it has been proved that pectin metabolism has a critical role in softening of most fruits, being pectin solubilisation a general characteristic of softening. The increase on pectins loosely bound to the cell wall as the fruit soften may be preceded by xyloglucan depolymerisation in some fruit, but, the physiological reasons for pectin solubilisation, as well as the link between this process and xyloglucan processing are far from clear.

AFM studies have demonstrate that this technique has unique advantages over other analytical procedures to characterize the nanostructure of cell wall polymers in a more natural context. Using this technique in combination with chemical or enzymatic hydrolysis of samples, new models for pectin structure have been proposed that incorporate novel characteristics found using this approach, i.e. the presence of GalA branches in the HG backbone or the aggregation of RGI and HG in micellar aggregates through RGII dimerisation. Although the number of AFM studies related to fruit ripening are still scarce, the AFM characterisation of cell walls isolated from fleshy fruits has provided a novel view of the modifications taking place in the pectic matrix during fruit ripening and postharvest. In general, these changes involve the loosening of the structural complexity of pectins as the fruit soften, i.e. individual pectin chains are shorter and less branched and the width of highly packed pectins is reduced. Additionally, the presence of micellar complexes in pectin samples from ripe fruits is also reduced, suggesting a lower tendency of pectins to self-aggregate. Postharvest treatments that extend fruit shelf life ameliorate these changes observed by AFM in some commodities. Overall, these results clearly link pectin structure and disassembly with fruit texture. Most of these AFM studies point at the pectin fraction extracted with sodium carbonate, supposedly located within the primary cell wall,

as the main determinant of softening. Additional work is needed to identify the physicochemical bases of the complex structures visualized by AFM.

In contrast to the extensive research on pectins performed in recent years, few AFM studies have focused in the characterization of hemicellulose and cellulose disassembly. Additionally, the results reported about these issues are not conclusive. This is, therefore, a field that need more research efforts in the future. One of the most promising applications of AFM is it's use as a nanoscale texturometer to measure cell wall strength, both in intact cells or in isolated cell walls. The application of nanomechanical studies to other fruit commodities and the refinement of the technique to get more consistent results could contribute significantly to acquire a deeper knowledge of the fruit softening process.

Acknowledgments

This work was funded by the Ministerio de Educación y Ciencia of Spain and Feder EU Funds (grant reference: AGL2014-55784-C2-1-R). SP was supported by a contract funded by the postdoctoral program of the University of Málaga (reference: E-29-2017-0215684). The research at IFR, currently Quandram Institute Bioscience, was supported through the BBSRC core grant to the Institute. We thank Andrew Kirby for his invaluable support and experience during our AFM training.

References

664 Airianah, O. B., Vreeburg, R. A., & Fry, S. C. (2016). Pectic polysaccharides are attacked by
665 hydroxyl radicals in ripening fruit: evidence from a fluorescent fingerprinting method. *Annals*
666 *of Botany*, *117*, 441-455.
667 Atkinson, R. G., Sutherland, P. W., Johnston, S. L., Gunaseelan, K., Hallett, I. C., Mitra, D., et
668 al. (2012). Down-regulation of POLYGALACTURONASE1 alters firmness, tensile strength
669 and water loss in apple (*Malus* x *domestica*) fruit. *BMC Plant Biology*, *12*, 129.
670 Bourne, M. C. (2002). *Food texture and viscosity: concept and measurement*. London: Academic
671 Press.
672 Brummell, D. A. (2006). Cell wall disassembly in ripening fruit. *Functional Plant Biology*, *33*,
673 103-119.
674 Brummell, D. A., & Harpster, M. H. (2001). Cell wall metabolism in fruit softening and quality
675 and its manipulation in transgenic plants. *Plant Molecular Biology*, *47*, 311-340.
676 Brummell, D. A., Harpster, M. H., Civello, P. M., Palys, J. M., Bennett, A. B., & Dunsmuir, P.
677 (1999). Modification of expansin protein abundance in tomato fruit alters softening and cell
678 wall polymer metabolism during ripening. *Plant Cell*, *11*, 2203-2216.
679 Brummell, D. A., Del Cin, V., Crisosto, C. H., & Labavitch, J. M. (2004). Cell wall metabolism
680 during maturation, ripening and senescence of peach fruit. *Journal of Experimental Botany*,
681 *55*, 2029-2039.
682 Burgert, I., & Keplinger, T. (2013). Plant micro- and nanomechanics: experimental techniques
683 for plant cell-wall analysis. *Journal of Experimental Botany*, *64*, 4635-4649.
684 Castellarin, S. D., Gambetta, G. A., Wada, H., Krasnow, M. N., Cramer, G. R., Peterlunger, E.,
685 et al. (2016). Characterization of major ripening events during softening in grape: turgor,

686 sugar accumulation, abscisic acid metabolism, colour development, and their relationship with
687 growth. *Journal of Experimental Botany*, *67*, 709-722.
688 Cárdenas-Pérez, S., Chanona-Pérez, J. J., Méndez-Méndez, J. V., Calderón-Domínguez, G.,
689 López-Santiago, R., & Arzate-Vázquez, I. (2016). Nanoindentation study on apple tissue and
690 isolated cells by atomic force microscopy, image and fractal analysis. *Innovative Food*
691 *Science and Emerging Technologies*, *34*, 234–242.
692 Cavalier, D. M., Lerouxel, O., Neumetzler, L., Yamauchi, K., Reinecke, A., Freshour, G., et al.
693 (2008). Disrupting two *Arabidopsis* thaliana xylosyltransferase genes results in plants
694 deficient in xyloglucan, a major primary cell wall component. *The Plant Cell*, *20*, 1519-1537.
695 Chen, F. S, Zhang, L. F., An, H. J., Yang, H. S., Sun, X. Y., Liu, H., et al. (2009). The
696 nanostructure of hemicellulose of crisp and soft Chinese cherry (*Prunus pseudocerasus* L.)
697 cultivars at different stages of ripeness. *LWT-Food Science and Technology*, *42*, 125-130.
698 Chen, F., Liu, H., Yang, H., Lai, S., Cheng, X., Xin, Y., et al. (2011). Quality attributes and cell
699 wall properties of strawberries (*Fragaria annanassa* Duch.) under calcium chloride treatment.
700 *Food Chemistry*, *126*, 450-459.
701 Chong, J. X., Lai, S., & Yang, H. (2015). Chitosan combined with calcium chloride impacts
702 fresh-cut honeydew melon by stabilising nanostructures of sodium-carbonate-soluble pectin.
703 *Food Control*, *53*, 195-205.
704 Chormova, D., Messenger, D. J., & Fry, S. C. (2014). Boron bridging of rhamnogalacturonan-II,
705 monitored by gel electrophoresis, occurs during polysaccharide synthesis and secretion but
706 not post-secretion. *Plant Journal*, *77*, 534-546.

Cybulska, J., Zdunek, A., Psonka-Antonczyk, K. M., & Stokke, B. T. (2013). The relation of apple texture with cell wall nanostructure studied using an atomic force microscope. *Carbohydrate Polymers*, *92*, 128-137.

Cybulska, J., Zdunek, A. & Koziol, A. (2015). The self-assembled network and physiological degradation of pectins in carrot cell walls. *Food Hydrocolloids*, *43*, 41-50.

Ding, S. Y., Liu, Y. S., Zeng, Y., Himmel, M. E., Baker, J. O., & Bayer, E. A. (2012). How does plant cell wall nanoscale architecture correlate with enzymatic digestibility?. *Science*, *338*, 1055-1060.

Eklöf, J. M., & Brumer, H. (2010). The XTH gene family: an update on enzyme structure, function, and phylogeny in xyloglucan remodelling. *Plant Physiology*, *153*, 456-466.

Gapper, N. E., McQuinn, R. P., & Giovannoni, J. J. (2013). Molecular and genetic regulation of fruit ripening. *Plant Molecular Biology*, *82*, 575-591.

Goulao, L. F., & Oliveira, C. M. (2008). Cell wall modification during fruit ripening: when a fruit is not the fruit. *Trends in Food Science & Technology*, *19*, 4-25.

Gunning, A. P., & Morris, V. J. (2017). Getting the feel of food structure with atomic force microscopy. *Food Hydrocolloids*, in press, http://dx.doi.org/10.1016/j.foodhyd.2017.05.017.

Han, Y., Han, S., Ban, Q., He, Y., Jin, M., & Rao, J. (2017). Overexpression of persimmon *DkXTH1* enhanced tolerance to abiotic stress and delayed fruit softening in transgenic plants. *Plant Cell Reports*, *36*, 583-896.

Harker, F. R., Stec, M. G. H., Hallett, I. C., & Bennett, C. L. (1997). Texture of parenchymatous plant tissue: a comparison between tensile and other instrumental and sensory measurements of tissue strength and juiciness. *Postharvest Biology and Technology*, *11*, 63-72.

729 Harris, P. J., & Smith, B. G. (2006). Plant cell walls and cell-wall polysaccharides: Structures,
730 properties and uses in food products. *International Journal of Food Science and Technology*,
731 *41*, 129-143.
732 Jiménez-Bermúdez, S., Redondo-Nevado, J., Muñoz-Blanco, J., Caballero, J. L., López-Aranda,
733 J. M., Valpuesta, V., et al. (2002). Manipulation of strawberry fruit softening by antisense
734 expression of a pectate lyase gene. *Plant Physiology*, *128*, 751-759.
735 Kafle, K., Xi, X., Lee, C. M., Tittmann, B. R., Cosgrove, D. J., Park, Y. B., & Kim, S. H. (2014).
736 Cellulose microfibril orientation in onion (*Allium cepa* L.) epidermis studied by atomic force
737 microscopy (AFM) and vibrational sum frequency generation (SFG)
738 spectroscopy. *Cellulose*, *21*, 1075-1086.
739 Kirby, A. R., MacDougall, A. J., & Morris, V. J. (2008). Atomic force microscopy of tomato and
740 sugar beet pectin molecules. *Carbohydrate Polymers*, *71*, 640-647.
741 Koh, T. H., Melton, L. D., & Newman, R. H. (1997). Solid-state 13C NMR characterization of
742 cell walls of ripening strawberries. C*anadian Journal of Botany-Revue Canadienne de*
743 *Botanique*, *75*, 1957-1964.
744 Koziol, A., Cybulska, J., Pieczywek, P. M., & Zdunek, A. (2015). Evaluation of structure and
745 assembly of xyloglucan from tamarind seed (*Tamarindus indica* L.) with atomic force
746 microscopy. *Food Biophysics*, *10*, 396-402.
747 Koziol A., Cybulska, J., Pieczywek, P. M., & Zdunek, A. (2017). Changes of pectin
748 nanostructure and cell wall stiffness induced in vitro by pectinase. *Carbohydrate Polymers*,
749 *161*, 197-207.

Lai, S., Chen, F., Zhang, L., Yang, H., Deng, Y., & Yang B. (2013). Nanostructural difference of water-soluble pectin and chelate-soluble pectin among ripening stages and cultivars of Chinese cherry. *Natural Product Research, 27*, 379-385.

Lesniewska, E., Adrian, M., Klinguer, A., & Pugin, A. (2004). Cell wall modification in grapevine cells in response to UV stress investigated by atomic force microscopy. *Ultramicroscopy*, *100*, 171-178.

Liu, H., Chen, F., Lai, S., Tao, J., Yang, H., & Jiao, Z. (2017). Effects of calcium treatment and low temperature storage on cell wall polysaccharide nanostructures and quality of postharvest apricot (*Prunus armeniaca*). *Food Chemistry*, *225*, 87-97.

Makshakova, O. N., Gorshkova, T. A., Mikshina, P. V., Zuev, Y. F., & Perez, S. (2017). Metrics of rhamnogalacturonan I with β-(1→4)-linked galactan side chains and structural basis for its self-aggregation. *Carbohydrate Polymers*, *158*, 93-101.

Matsunaga, T., Ishii, T., Matsumoto, S., Higuchi, M., Darvill, A., Albersheim, P., & O'Neill, M. A. (2004). Occurrence of the primary cell wall polysaccharide rhamnogalacturonan II in pteridophytes, lycophytes, and bryophytes. Implications for the evolution of vascular plants. *Plant Physiology*, *134*, 339–351.

Maxwell, E. G., Belshaw, N. J., Waldron, K. W., & Morris, V. J. (2012). Pectin – An emerging new bioactive food polysaccharide. *Trends in Food Science & Technology*, *24*, 64–73.

McIntire, T. M., & Brant, D. A. (1999). Imaging of carrageenan macrocycles and amylose using noncontact atomic force microscopy. *International Journal of Biological Macromolecules*, *26*, 303-310.

771 Mercado, J. A., Pliego-Alfaro, F., & Quesada, M. A. (2011). Fruit shelf life and potential for its
772 genetic improvement. In M. A. Jenks, & P. J. Bebeli (Eds.), *Breeding for Fruit Quality* (pp.
773 81-104). Oxford: John Wiley & Sons.
774 Miedes, E., Herbers, K., Sonnewald, U., & Lorences, E. P. (2010). Overexpression of a cell wall
775 enzyme reduces xyloglucan depolymerization and softening of transgenic tomato fruits.
776 *Journal of Agricultural Food Chemistry*, *58*, 5708-2713.
777 Mierczyńska, J., Cybulska, J., & Zdunek, A. (2017). Rheological and chemical properties of
778 pectin enriched fractions from different sources extracted with citric acid. *Carbohydrate*
779 *Polymers*, *156*, 443-451.
780 Minoia, S., Boualem, A., Marcel, F., Troadec, C., Quemener, B., Cellini, F., et al. (2016).
781 Induced mutation in tomato SlExp1 alter cell wall metabolism and delay fruit softening. *Plant*
782 *Science*, *242*, 195-202.
783 Molina-Hidalgo, F. J., Franco, A. R., Villatoro, C., Medina-Puche, L., Mercado, J. A., Hidalgo,
784 M. A., et al. (2013). The strawberry (*Fragaria* × *ananassa*) fruit-specific
785 rhamnogalacturonate lyase 1 (*FaRGLyase1*) gene encodes an enzyme involved in the
786 degradation of cell-wall middle lamellae. *Journal of Experimental Botany*, *64*, 1471-1483.
787 Morris, V. J., Kirby, A. R., & Gunning, A. P. (2010). *Atomic force microscopy for biologists*.
788 London: Imperial College Press.
789 Morris, V. J., Gromer, A., Kirby, A. R., Bongaerts, R. J. M., & Patrick Gunning, A. (2011).
790 Using AFM and force spectroscopy to determine pectin structure and (bio) functionality.
791 *Food Hydrocolloids*, *25*, 230-237.

792 Munarin, F., Guerreiro, S. G., Grellier, M. A., Tanzi, M. C., Barbosa, M. A., Petrini, P., &
793 Granja, P. L. (2011). Pectin-based injectable biomaterials for bone tissue
794 engineering. *Biomacromolecules*, *12*, 568-577.
795 Neves, S. C., Gomes, D. B., Sousa, A., Bidarra, S. J., Petrini, P., Moroni, L., et al. (2015).
796 Biofunctionalized pectin hydrogels as 3D cellular microenvironments. *Journal of Materials*
797 *Chemistry B*, *3*, 2096-2108.
798 Newman, R. H., & Redgwell, R. J. (2002). Cell wall changes in ripening kiwifruit: 13 C solid
799 state NMR characterisation of relatively rigid cell wall polymers. *Carbohydrate Polymers*, *49*,
800 121-129.
801 Ng, J. K. T., Zujovic, Z. D., Smith, B. G., Johnston, J. W., Schröder, R., & Melton, L. D. (2014).
802 Solid-state 13C NMR study of the mobility of polysaccharides in the cell walls of two apple
803 cultivars of different firmness. *Carbohydrate Research*, *386*, 1–6.
804 Ng, J. K. T., Schröder, R., Brummell, D. A., Sutherland, P. W., Hallett, I. C., Smith, B., G., et al.
805 (2015). Lower cell wall pectin solubilisation and galactose loss during early fruit development
806 in apple (*Malus* x *domestica*) cultivar 'Scifresh' are associated with slower softening rate.
807 *Journal of Plant Physiology*, *176*, 129-137.
808 Niimura, H., Yokoyama, T., Kimura, S., Matsumoto, Y., & Kuga, S. (2010). AFM observation
809 of ultrathin microfibrils in fruit tissues. *Cellulose*, *17*, 13-18.
810 Oliveira, T. Í. S., Rosa, M. F., Ridout, M. J., Cross, K., Brito, E. S., Silva, L. M., et al. (2017).
811 Bionanocomposite films based on polysaccharides from banana peels. *International Journal*
812 *of Biological Macromolecules*, *101*, 1-8.

O'Neill, M. A., Ishii, T., Albersheim, P., & Darvill, A. G. (2004). Rhamnogalacturonan II: Structure and function of a borate cross-linked cell wall pectic polysaccharide. *Annual Review of Plant Biology*, *55*, 109–139.

Ovodova, R. G., Popov, S. V., Bushneva, O. A., Golovchenko, V. V., Chizhov, A. O., Klinov, D. V., et al. (2006). Branching of the galacturonan backbone of comaruman, a pectin from the marsh cinquefoil *Comarum palustre* L. *Biochemistry*, *71*, 538-542.

Paniagua, C., Pose, S., Morris, V. J., Kirby, A. R., Quesada, M. A., & Mercado, J. A. (2014). Fruit softening and pectin disassembly: an overview of nanostructural pectin modifications assessed by atomic force microscopy. *Annals of Botany*, *114*, 1375-1383.

Paniagua, C., Blanco-Portales, R., Barceló-Muñoz, M., García-Gago, J. A., Waldron, K. W., Quesada, et al. (2016). Antisense down-regulation of the strawberry β-galactosidase gene *FaβGal4* increases cell wall galactose levels and reduces fruit softening. *Journal of Experimental Botany*, *67*, 619-631.

Paniagua, C., Kirby, A. R., Gunning, A. P., Morris, V. J., Matas, A. J., Quesada, M. A., et al. (2017a). Unravelling the nanostructure of strawberry fruit pectins by endo-polygalacturonase digestion and atomic force microscopy. *Food Chemistry*, *224*, 270-279.

Paniagua, C., Santiago-Doménech, N., Kirby, A. R., Gunning, A. P., Morris, V. J., Quesada, M. A., et al. (2017b). Structural changes in cell wall pectins during strawberry fruit development. *Plant Physiology and Biochemistry*, *118*, 55-63.

Park, Y. B., & Cosgrove, D. J. (2012). A revised architecture of primary cell walls based on biomechanical changes induced by substrate-specific endoglucanases. *Plant Physiology*, *158*, 1933-1943.

835 Peaucelle, A., Braybrook, S. A., Le Guillou, L., Bron, E., Kuhlemeier, C., & Hofte, H. (2011).
836 Pectin-induced changes in cell wall mechanics underlie organ initiation in *Arabidopsis*.
837 *Current Biology*, *21*, 1720-1726.
838 Percy, A. E., Melton, L.D., & Jameson, P.E. (1997). Xyloglucan and hemicelluloses in the cell
839 wall during apple fruit development and ripening. *Plant Science*, *125*, 31-39.
840 Pieczywek, P.M., Koziol, A., Konopacka, D., Cybulska, J., & Zdunek, A. (2017). Changes in
841 cell wall stiffness and microstructure in ultrasonically treated apple. *Journal of Food*
842 *Engineering*, *197*, 1-8.
843 Posé, S., Kirby, A. R., Mercado, J. A., Morris, V. J., & Quesada, M. A. (2012). Structural
844 characterization of cell wall pectin fractions in ripe strawberry fruits using AFM.
845 *Carbohydrate Polymers*, *88*, 882–890.
846 Posé, S., Paniagua, C., Cifuentes, M., Blanco-Portales, R., Quesada, M. A., & Mercado, J. A.
847 (2013). Insights into the effects of polygalacturonase *FaPG1* gene silencing on pectin matrix
848 disassembly, enhanced tissue integrity, and firmness in ripe strawberry fruits. *Journal of*
849 *Experimental Botany*, *64*, 3803–3815.
850 Pose, S., Kirby, A. R., Paniagua, C., Waldron, K. W., Morris, V. J., Quesada, M. A., et al.
851 (2015). The nanostructural characterization of strawberry pectins in pectate lyase or
852 polygalacturonase silenced fruits elucidates their role in softening. *Carbohydrate Polymers*,
853 *132*, 134-145.
854 Prasanna, V., Prabha, T.N., & Tharanathan, R.N. (2007). Fruit ripening phenomena - An
855 overview. *Critical Reviews in Food Science and Nutrition*, *47*, 1-19.
856 Quesada, M. A., Blanco-Portales, R., Pose, S., García-Gago, J. A., Jiménez-Bermúdez, S.,
857 Muñoz-Serrano, A., et al. (2009). Antisense down-regulation of the *FaPG1* gene reveals an

858 unexpected central role for polygalacturonase in strawberry fruit softening. *Plant Physiology*,
859 *150*, 1022-1032.
860 Redgwell, R. J., Melton, L. D., & Brasch, D. J. (1992) Cell wall dissolution in ripening kiwifruit
861 (*Actinidia deliciosa*): solubilisation of the pectic polymers. *Plant Physiology*, *98*, 71-81.
862 Redgwell, R. J., MacRae, E. A., Hallett, I., Fischer, M., Perry, J., & Harker, R. (1997a). In vivo
863 and in vitro swelling of cell walls during fruit ripening. *Planta*, *203*, 162-173.
864 Redgwell, R.J., Fischer, M., Kendall, E., MacRae, E.A., Perry, J., & Harker, R. (1997b).
865 Galactose loss and fruit ripening: high-molecular-weight arabinogalactans in the pectic
866 polysaccharides of fruit cell walls. *Planta*, *203*, 174-181.
867 Rose, J. K. C., Hadfield, K. A., Labavitch, J. M., & Bennett, A. B. (1998) Temporal sequence of
868 cell wall disassembly in rapidly ripening melon fruit. *Plant Physiology*, *117*, 345-361.
869 Rosli, H. G., Civello, P. M., & Martinez, G. A. (2004). Changes in cell wall composition of three
870 *Fragaria* x *ananassa* cultivars with different softening rate during ripening. *Plant Physiology*
871 *and Biochemistry*, *42*, 823-831.
872 Round, A. N., MacDougall, A. J., Ring, S. G., & Morris, V. J. (1997). Unexpected branching in
873 pectin observed by atomic force microscopy. *Carbohydrate Research*, *303*, 251-253.
874 Round, A. N., Rigby, N. M., MacDougall, A. J., Ring, S. G., & Morris, V. J. (2001).
875 Investigating the nature of branching in pectin by atomic force microscopy and carbohydrate
876 analysis. *Carbohydrate Research*, *331*, 337-342.
877 Round, A. N., Rigby, N. M., MacDougall, A. J., & Morris, V. J. (2010). A new view of pectin
878 structure revealed by acid hydrolysis and atomic force microscopy. *Carbohydrate Research*,
879 *345*, 487–497.

880 Routier-Kierzkowska, A. L., Weber, A., Kochova, P., Felekis, D., Nelson, B. J., Kuhlemeier, C.,
881 et al. (2012). Cellular force microscopy for in vivo measurements of plant tissue mechanics.
882 *Plant Physiology*, *158*, 1514-1522.
883 Saladié, M., Matas, A. J., Isaacson, T., Jenks, M. A, Goodwin, S. M., Niklas, K. J., et al. (2007).
884 A reevaluation of the key factors that influence tomato fruit softening and integrity. *Plant*
885 *Physiology*, *144*, 1012-1028.
886 Santiago-Doménech, N., Jiménez-Bermúdez, S., Matas, A. J., Rose, J. K. C., Muñoz-Blanco, J.,
887 Mercado, J. A., et al. (2008). Antisense inhibition of a pectate lyase gene supports a role for
888 pectin depolymerization in strawberry fruit softening. *Journal of Experimental Botany*, *59*,
889 2769-2779.
890 Scheller, H. K., & Ulvskov, P. (2010). Hemicelluloses. *Annual Review of Plant Biology*, *61*, 263-
891 289.
892 Shiga, T. M., Fabi, J. P., do Nascimento, J. R., Petkowicz, C. L., Vriesmann, L. C., Lajolo, F.M.,
893 et al. (2009). Changes in cell wall composition associated to the softening of ripening papaya:
894 evidence of extensive solubilization of large molecular mass galactouronides. *Journal of*
895 *Agricultural and Food Chemistry*, *57*, 7064-7071.
896 Sila, D. N., Van Buggenhout, S., Duvetter, T., Fraeye, I., De Roeck, A., Van Loey, A., &
897 Hendrickx, M. (2009). Pectins in processed fruits and vegetables: part II-structure-function
898 relationships. *Comprehensive Reviews in Food Science and Food Safety*, *8*, 86-104.
899 Thimm, J. C., Burritt, D. J., Ducker, W. A., & Melton, L. D. (2009). Pectins influence microfibril
900 aggregation in celery cell walls: An atomic force microscopy study. *Journal of Structural*
901 *Biology*, *168*, 337-344.

902 Toivonen, P. M. A., & Brummell, D. A. (2008). Biochemical bases of appearance and texture
903 changes in fresh-cut fruit and vegetables. *Postharvest Biology and Technology*, *48*, 1-14.
904 Uluisik, S., Chapman, N. H., Smith, R., Poole, M., Adams, G., Gillis, R. B., et al. (2016).
905 Genetic improvement of tomato by targeted control of fruit softening. Nature Biotechnology,
906 34, 950-952.
907 Van Buggenhout, S., Sila, D. N., Duvetter, T., Van Loey, A., & Hendrickx, M. (2009). Pectins in
908 processed fruits and vegetables: part III-texture engineering. *Comprehensive Reviews in Food*
909 *Science and Food Safety*, *8*, 105–117.
910 Vicente, A. R., Saladié, M., Rose, J. K. C., & Labavitch, J. M. (2007a). The linkage between cell
911 wall metabolism and fruit softening: looking to the future. *Journal of the Science of Food and*
912 *Agriculture*, *87*, 1435-1448.
913 Vicente, A. R., Ortugno, C., Powell, A. L. T., Greve, L. C., & Labavitch, J. M. (2007b).
914 Temporal sequence of cell wall disassembly events in developing fruits. 1. Analysis of
915 raspberry (*Rubus idaeus*). *Journal of Agricultural and Food Chemistry*, *55*, 4119-4124
916 Vincken, J. P., Schols, H. A., Oomen, R. J. F. J., McCann, M. C., Ulvskov, P., Voragen, A. G. J.,
917 et al. (2003). If homogalacturonan were a side chain of rhamnogalacturonan I. Implications
918 for cell wall architecture. *Plant Physiology*, *132*, 1781-1789.
919 Voragen, A. G. J., Coenen, G.-J., Verhoef, R. P., & Schols, H. A. (2009). Pectin, a versatile
920 polysaccharide present in plant cell walls. *Structural Chemistry*, *20*, 263-275.
921 Wang, H., Chen, F., Yang, H., Chen, Y., Zhang, L., & An, H. (2012). Effects of ripening stage
922 and cultivar on physicochemical properties and pectin nanostructures of jujubes.
923 *Carbohydrate Polymers*, *89*, 1180-1188.

924 Wang, T., Park, Y. B., Cosgrove, D. J., & Hong, M. (2015). Cellulose-pectin spatial contacts are
925 inherent to never-dried *Arabidopsis* primary cell walls: evidence from solid-state nuclear
926 magnetic resonance. *Plant Physiology*, *168*, 871-884.
927 Wen, B., Ström, A., Tasker, A., West, G., & Tucker, G. A. (2013). Effect of silencing the two
928 major tomato fruit pectin methylesterase isoforms on cell wall pectin metabolism. *Plant*
929 *Biology*, *15*, 1025-1032.
930 Willats, W. G. T., McCartney, L., Mackie, W., & Knox, J. P. (2001). Pectin: Cell biology and
931 prospects for functional analysis. *Plant Molecular Biology, 47*, 9–27.
932 Xi, X., Kim, S. H., & Tittmann, B. (2015). Atomic force microscopy based nanoindentation
933 study of onion abaxial epidermis walls in aqueous environment. *Journal of Applied Physics*,
934 *117*, 24703.
935 Xin, Y., Chen, F., Yang, H., Zhang, P., Deng, Y., & Yang, B. (2010). Morphology, profile and
936 role of chelate-soluble pectin on tomato properties during ripening. *Food Chemistry*, *121*,
937 372-380.
938 Xin, F., Chen, F., Lai, S., & Yang, H. (2017). Influence of chitosan-based coatings on the
939 physicochemical properties and pectin nanostructure of Chinese cherry. *Postharvest Biology*
940 *and Technology*, *133*, 64-71.
941 Yang, H., An, H., Feng, G., Li, Y., & Lai, S. (2005). Atomic force microscopy of the water-
942 soluble pectin of peaches during storage. *European Food Research and Technology*, *220*,
943 587-591.
944 Yang, H., Lai, S., An, H., & Li, Y. (2006a). Atomic force microscopy study of the ultrastructural
945 changes of chelate-soluble pectin in peaches under controlled atmosphere storage. *Postharvest*
946 *Biology and Technology*, *39*, 75-83.

947 Yang, H.-S., Feng, G.-P., An, H.-J., & Li, Y.-F. (2006b). Microstructure changes of sodium
948 carbonate-soluble pectin of peach by AFM during controlled atmosphere storage. *Food*
949 *Chemistry*, *94*, 179-192.
950 Yang, H., Chen, F., An, H., & Lai, S. (2009). Comparative studies on nanostructures of three
951 kinds of pectins in two peach cultivars using atomic force microscopy. *Postharvest Biology*
952 *and Technology*, *51*, 391-398.
953 Yang, H., Wu, Q., Ng, L. Y., & Wang, S. (2017). Effects of vacuum impregnation with calcium
954 lactate and pectin methylesterase on quality attributes and chelate-soluble pectin morphology
955 of fresh-cut papayas. *Food and Bioprocess Technology*, *10*, 901-913.
956 Yapo, B. M. (2011a). Pectic substances: From simple pectic polysaccharides to complex pectins
957 -A new hypothetical model. *Carbohydrate Polymers*, *86*, 373-385.
958 Yapo, B. M. (2011b). Rhamnogalacturonan-I: a structurally puzzling and functionally versatile
959 polysaccharide from plant cell walls and mucilages. *Polymer Reviews*, *51*, 391-413.
960 Yoshioka, H., Hayama, H., Tatsuki M., & Nakamura, Y. (2011). Cell wall modifications during
961 softening in melting type peach “Akatsuki” and non-melting type peach “Mochizuki”.
962 *Postharvest Biology and Technology*, *60*, 100-110.
963 Zareie, M. H., Gokmen, V., & Javadipour, I. (2003). Investigating network, branching, gelation
964 and enzymatic degradation in pectin by atomic force microscopy. *Journal of Food Science*
965 *and Technology*, *40*, 169-172.
966 Zdunek, A., & Kurenda, A. (2013). Determination of the elastic properties of tomato fruit cells
967 with an atomic force microscope. *Sensors*, *13*, 12175-12191.

968 Zdunek, A., Koziol, A., Pieczywek, P. M., Cybulska, J. (2014). Evaluation of the nanostructure
969 of pectin, hemicellulose and cellulose in the cell walls of pears of different texture and
970 firmness. *Food and Bioprocess Technology*, *7*, 3525-3535.
971 Zdunek, A., Koziol, A., Cybulska, J., Lekka, M. & Pieczywek, P. M. (2016). The stiffening of
972 the cell walls observed during physiological softening of pears. *Planta*, *243*, 519-529.
973 Zhang, L., Chen, F., An, H., Yang, H., Sun, X., Guo, X., et al. (2008). Physicochemical
974 properties, firmness, and nanostructures of sodium carbonate-soluble pectin of 2 chinese
975 cherry cultivars at 2 ripening stages. *Journal of Food Science*, *73*, N17-N22.
976 Zhang, L., Chen, F., Yang, H., Sun, X., Liu, H., Gong, X., et al. (2010). Changes in firmness,
977 pectin content and nanostructure of two crisp peach cultivars after storage. *LWT-Food Science*
978 *and Technology*, *43*, 26-32.
979 Zhang, L., Chen, F., Yang, H., Ye, X., Sun, X., Liu, D., et al. (2012). Effects of temperature and
980 cultivar on nanostructural changes of water-soluble and chelate-soluble pectin in peaches.
981 *Carbohydrate Polymers*, *87*, 816-821.
982 Zhang, T., Zheng, Y. Z., & Cosgrove, D. J. (2016). Spatial organization of cellulose microfibrils
983 and matrix polysaccharides in primary plant cell walls as imaged by multichannel atomic
984 force microscopy. *Plant Journal*, *85*, 179-192.
985 Zhang, Z., Wang, N., Jiang, S., Xu, H., Wang, Y., Wang, C., et al. (2017a). Analysis of the
986 xyloglucan endotransglucosylase/hydrolase gene family during apple fruit ripening and
987 softening. *Journal of Agricultural and Food Chemistry*, *65*, 429-434.
988 Zhang, L., Chen, F., Zhang, P., Lai, S., & Yang, H. (2017b). Influence of rice bran wax coating
989 on the physicochemical properties and pectin nanostructure of cherry tomatoes. *Food and*
990 *Bioprocess Technology*, *10*, 349-357.

991 Zykwinska, A., Thibault, J. F., & Ralet, M. C. (2008). Competitive binding of pectin and
992 xyloglucan with primary cell wall cellulose. *Carbohydrate Polymers*, *74*, 957-961.

993

ACCEPTED MANUSCRIPT

994 **Figure legends**

995

996 **Fig. 1.** Main processes leading to textural changes during ripening and postharvest storage of
997 fleshy fruit. Ara: arabinose; Gal: galactose; XyG: xyloglucans.

998

999 **Fig. 2.** Schematic overview of main applications of AFM to the study of the cell wall
1000 disassembly process during fruit ripening and postharvest. HGA: homogalacturonan; RGI:
1001 rhamnogalacturonan I.

1002

1003 **Fig. 3.** (A) AFM topographical image representative of strawberry Na_2CO_3 soluble pectins at
1004 ripe developmental stage from a transgenic line with a polygalacturonase gene downregulated.
1005 Inlets show zoomed areas representing micellar aggregates (B), linear chains (*) and branched
1006 chains (>) (C). 3D representation of pectin aggregates (D), and linear and branched chains (E).
1007 Scale bars are 100 nm (A) and 50 nm (B,C).

1008

1009 **Fig. 4.** (A) Representative image of CDTA pectins from strawberry ripe fruit obtained by AFM
1010 in contact mode. Branched pectin chains and micellar aggregates with emerging strands can be
1011 observed in the image. (B) Height profiles, showing the heights in a true branch point (black
1012 arrow) of a polymer chain (profile 1) and micellar aggregates (profile 2) with emerging strands
1013 of same height than isolated chains (grey arrow) and higher height at the core area (arrowhead).
1014 (Reprinted from Pose et al. (2015) with permission from Elsevier).

1015

Fig. 5. AFM topographical images of strawberry CDTA soluble pectin at unripe developmental stage. A) Pectin supramolecules of long fibrous appearance that involves some aggregation degree. B) Individual pectin molecules including isolated linear chains, branched chains and micellar aggregates. 3D representation of pectin supramolecules or aggregates, with higher heights at branch points (white arrows) (C) and individual pectin molecules (D). Scale bars: 100 nm.

ACCEPTED MANUSCRIPT

ACCEPTED MANUSCRIPT

Table 1. Quantitative AFM data of nano-structural features of cell wall polymers from several fruits during ripening and postharvest.

Fruit (*specie*)	Variety	Fruit stage	Cell wall fraction	Chain length (nm)	Other nanoproperties*	Reference
Apricot (*Prunus armeniaca* L.)	'Jinhong'	Harvest	WSP CSP HC	500 - >4000 <500 – 3500 <50 - >300	31 – 250 W 35 – 234; 34 %B 23 – 39 W; Net-like	Liu et al. (2017)
		Postharvest	WSP CSP HC	<500 - <4000 <500 – 3500 <50 – 300	12 – 70 W 12 – 47 W; 16%B 16 – 39 W; isolated chains	
Cherry (*Prunus pseudocerasus* L.)	'Caode' 'Bende'	Unripe	WSP CSP	ND ND	76-176 W 37-61 W	Lai *et al.* (2013)
			SSP	448-749	37-140 W	Zhang *et al.* (2008)
			HC	2000-5000	ND	Chen et al., 2009
		Ripe	WSP CSP	ND ND	37-82 W 17-55 W	Lai *et al.* (2013)
			SSP	123-749	37-140 W	Zhang *et al.* (2008)
			HC	2000-5000	ND	Chen et al., 2009
		Harvest	SSP	Network	30 - >110 W	Xin et al 2017
		Postharvest	SSP	Network	<30 – 50 W	
Jujube (*Zizyphus jujuba*)	'Huanghua' 'Zhanhua'	Unripe	CSP SSP	500, >3000 500, >3000	23-98 W 35-156 W	Wang *et al.* (2012)
		Ripe	CSP SSP	<500, >3000 <500, 2500	16-78 W 16-78 W	
Peach (*Prunus persica* L. Batsch.)	'Jinxiu'	Ripe	WSP	300-4200	20-100 W	Yang *et al.* (2009)

	'Milu'		CSP SSP	100-3000 20-900	ND 35-70 W	
	'Cangfangzaosheng' 'Songsenzaosheng'		WSP CSP	ND ND	91-217 W 91-181 W	Zhang et al (2012)
	'Jinxiu'	Harvest	WSP CSP SSP	ND	59 - 98W; 1.2 - 1.8H 20-156 W; 0.7-2.2 H 35-70 W; 3-5 H	Yang et al (2005; 2006a; 2006b)
		Postharvest	WSP CSP SSP	ND	12 -35 W; 0.9 - 1.2H 18-59 W; 0.5-2.3 H 12-66 W; 1.3-2.2 H	
	ND	Ripe	CWR	ND	1-2 ϕ	Niimura et al (2010)
Strawberry (*Fragaria* x *annanassa* Duch.)	'Chandler'	Unripe	CSP SSP	25-533 9-305	13 %B 20 %B	Paniagua et al. (2017b)
		Ripe	CSP SSP	18-277 10-255	3 %B 3 %B	
	'Shijixiang'	Ripe	WSP CSP SSP	88-3043 ND 87-1152	23-78 W 23-78 W 23-59 W	Chen *et al.* (2011)
	Unknown	Ripe	CWR	ND	1-2 ϕ	Niimura et al (2010)
Tomato (*Lycopersicon esculentum* Mill.)	'Rutger'	Unripe	CSP	40-560	ND	Kirby *et al.* (2008)
			SSP	20-400	ND	Round *et al.* (2010)
	'Dongsheng' 'Geruisi'	Turning	CSP	ND	19-117 W	Xin *et al.* (2010)
		Ripe	CSP	ND	15-117 W	
	'Mali'	Harvest	CSP	ND	15 – 250 W	Zhang et al 2017
		Postharvest	CSP	1000 - 5000	<50 – >200 W	

ACCEPTED MANUSCRIPT

Pear (*Pyrus communis* L.)	'Conference'	Harvest	WSP CSP SSP HC CWR	Aggregated ND ND 20-400 ND	0.2-1.5 H; 15-80 ϕ 0.1-1.5 H; 5.6 %B 0.1-2 H; 8.2 %B 0.4-8 H 23 ϕ	Zdunek et al., 2014
	'Xenia'	Harvest	WSP CSP SSP HC CWR	Aggregated ND Network 80 – 400 ND	0.2-1.5 H; 15-80 ϕ 0.1-2 H; 6.2 %B ND 0.1-3 H 23 ϕ	
Apple (*Malus x domestica* Borkh.)	'Honeycrisp'	Harvest	CWR	ND	38 ϕ	Cybulska et al., 2013
	'Mutsu'		CWR	ND	33 ϕ	
	'Cortland', 'Ligol', 'Rubin', 'Jonagold'		CWR	ND	26-28 ϕ	
Melon (*Cucumis melo L.*)	'Inodorus'	Harvest	SSP	200 - >700	21 - >70 W	Chong et al (2015)
		Postharvest	SSP	<100 - 500	<20 – 40 W	
Papaya (*Carica papaya L.*)	'Sekaki'	Harvest	CSP	ND	15 – 104 W	Yang et al (2017)
		Postharvest	CSP	ND	15 – 64 W	

ND: not described; WSP, CSP and SSP correspond to water-, chelated- and sodium carbonate-soluble pectins, respectively; HC: hemicellulose; CWR: cell wall residue, mainly composed of cellulose.
*H: height (nm); W: width (nm); %B: branching percentage; ϕ: diameter (nm).

ACCEPTED MANUSCRIPT

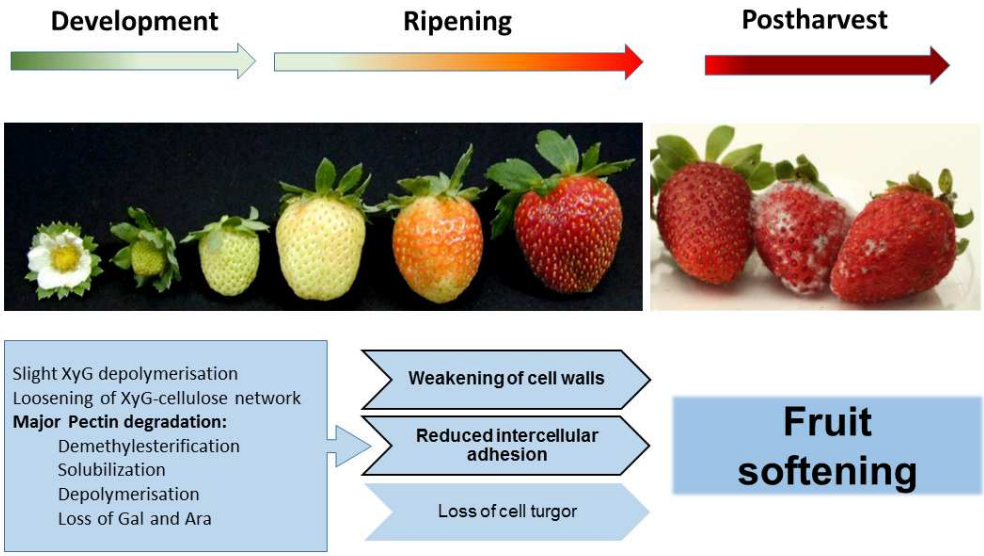

ACCEPTED MANUSCRIPT

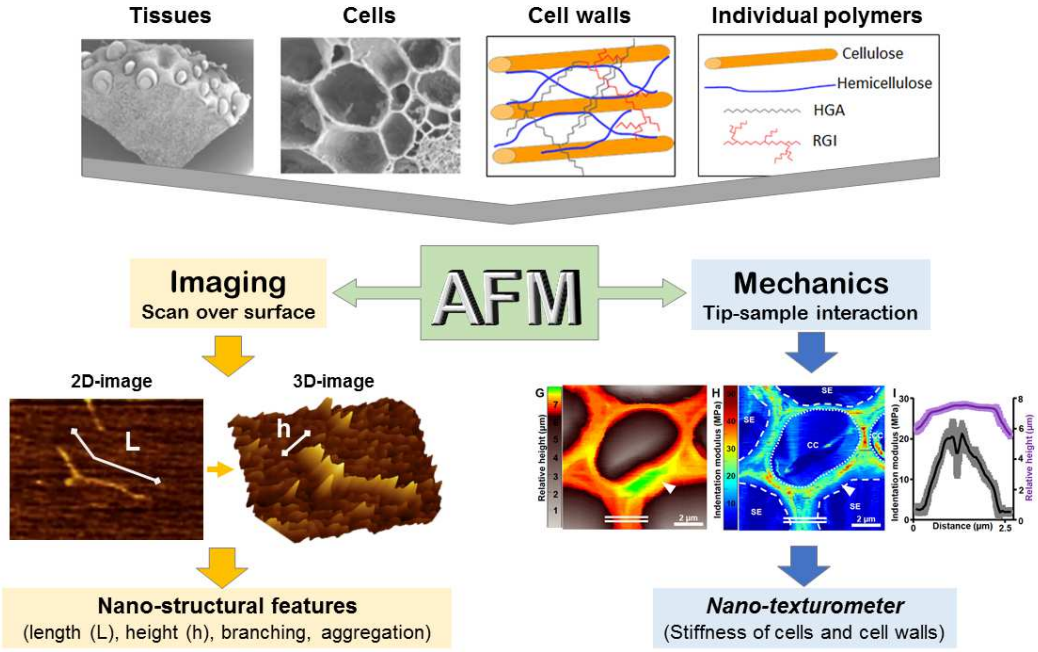

ACCEPTED MANUSCRIPT

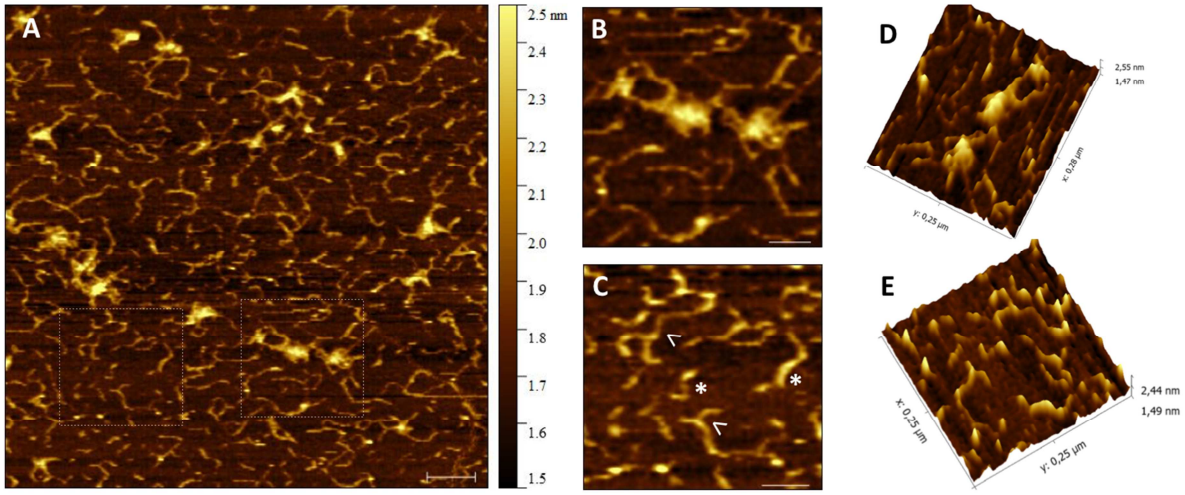

ACCEPTED MANUSCRIPT

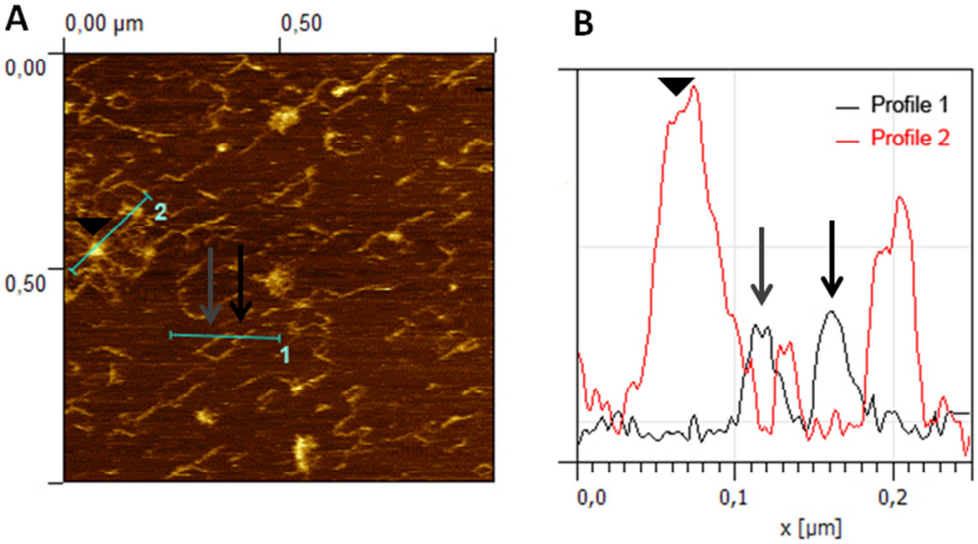

ACCEPTED MANUSCRIPT

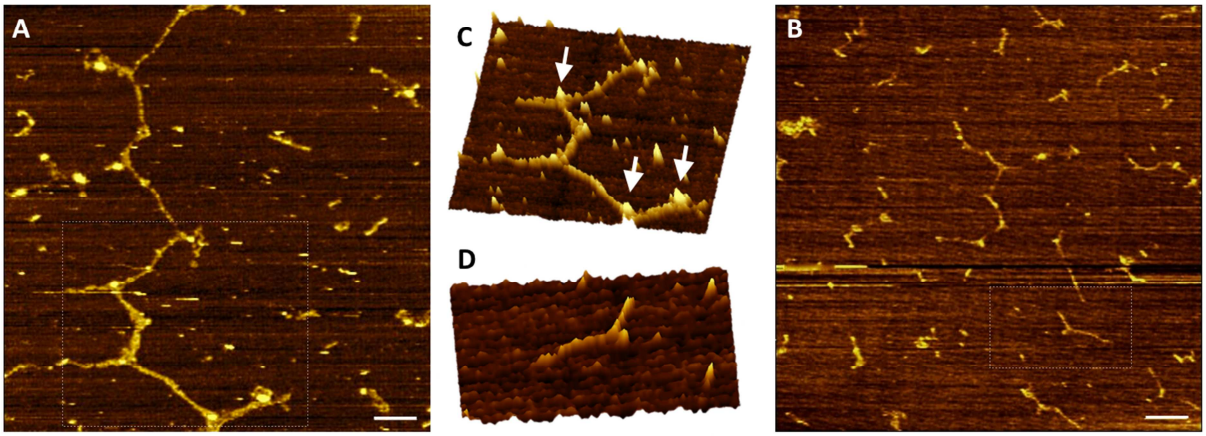

ACCEPTED MANUSCRIPT

ACCEPTED MANUSCRIPT

Highlights

1. Cell wall disassembly and loss of middle lamella occurs during fruit softening

2. Nanostructural properties of wall components can be characterized by AFM

3. A loss of pectin complexity, length and branching, correlates with softening

4. Postharvest treatments that reduce softening preserve pectin structure

5. AFM visualization of cellulose and hemicellulose is strongly influenced by the extraction procedure

ACCEPTED MANUSCRIPT